POTENTIAL FOR AEROBIC METHANOGENESIS IN NUTRIENT LIMITED INTERTIDAL

SEDIMENTS

by

ANGELICA MARIE DZIURZYNSKI

(Under the Direction of Samantha B. Joye)

ABSTRACT

Intertidal wetlands are dynamic systems that have variable nutrient regimes and biogeochemical gradients. Large reservoirs of methane exist in marsh sediments, but the microbial drivers of methane emissions from these coastal habitats are unconstrained. Cyanobacteria in salt marsh microbial mats may carry out aerobic methanogenesis to acquire essential nutrients under nutrient limited conditions. Nutrient amended treatments were analyzed under light and dark conditions to evaluate the microbial responses. Marine metagenomic approaches were used to further constrain the metabolic potential of intertidal cyanobacteria to express the functional genes required of this aerobic process. This study collectively advances our understanding of microbially-mediated coastal aerobic methane production in a changing climate.

POTENTIAL FOR AEROBIC METHANOGENESIS IN NUTRIENT LIMITED INTERTIDAL

SEDIMENTS

by

ANGELICA MARIE DZIURZYNSKI

BS, University of New Hampshire, 2022

A Non-Thesis Report Submitted to the Graduate Faculty of The University of Georgia in Partial

Fulfillment of the Requirements for the Degree

MASTER OF SCIENCE

ATHENS, GEORGIA

2024

POTENTIAL FOR AEROBIC METHANOGENESIS IN NUTRIENT LIMITED INTERTIDAL

SEDIMENTS

by

ANGELICA MARIE DZIURZYNSKI

Major Professor: Dr. Samantha B. Joye

Committee: Dr. Patricia M. Medeiros

                     Dr. Steven M. Holland

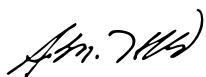*Signature*   *Date*

                                                     18 November 2024

Dr. Samantha B. Joye

Patricia Medeiros   18 November 2024

Dr. Patricia M. Medeiros

                                                     18 November 2024

Dr. Steven M. Holland

ACKNOWLEDGEMENTS

TABLE OF CONTENTS

CHAPTER 1

INTRODUCTION AND LITERATURE REVIEW

Documenting the controls of microbially-mediated carbon cycling are imperative to understand as the climate changes. Methane (CH_4) is a potent greenhouse gas with a warming potential more than 21 times that of carbon dioxide (Holmes et al., 2013). Rising atmospheric methane concentrations driven by anthropogenic sources account for roughly 20% of modern-day climate warming (Holmes et al., 2013; Lashof and Ahuja, 1990; Nisbet et al., 2014). While anthropogenic inputs make up a majority of atmospheric greenhouse gas emissions, natural sources of methane account for about a third of global emissions (Saunois et al., 2020). Most natural inputs of methane are from terrestrial sources, such as wetlands and inland waters (Bastviken et al., 2011). However, tidal wetlands play a critical role in natural methane cycling and they exhibit dynamic biogeochemical patterns.

Methane production occurs via biological methanogenesis as the terminal step of organic matter decomposition under strictly anoxic conditions, such as those found in deep sea and coastal sediments, saturated soils, and rice paddies. Methane is undersaturated in most of the oceans as it is consumed by microorganisms within sediments and in the water column (Joye, 2020). These microbial controls of methane fluxes to the atmosphere help regulate the global methane cycle.

Methane can be supersaturated with respect to atmospheric equilibrium in oceanic mixed layers (Lamontagne et al., 1973). Because classic methanogenesis is an anoxic process and therefore should not occur in oxygen-rich waters, this supersaturation in oxic surface waters has been dubbed the "oceanic methane paradox." Mixed layer methane supersaturation has been documented in ocean gyres, Arctic waters, and lakes (Karl et al., 2008; Damm et al., 2010; Bižić et al., 2019). Surface methane maxima are commonly associated with the deep chlorophyll maximum, indicating that there could be a potential biological source of this methane (Arx et al., 2023).

Nutrient limitation in surface oceans may play a pivotal role in the methane paradox. Phosphorus and nitrogen are two important macronutrients for aquatic microbes, but there are areas in the ocean where these nutrients are present in low concentrations and microbes must scavenge them. Microorganisms can use alternative cellular pathways to acquire essential nutrients in nutrient depleted, oxic surface waters (Karl et al., 2008; Repeta et al., 2016).

In phosphorus limited regions, methylphosphonate (MPn) can be demethylated by microbes to acquire phosphorus, whereas in nitrogen limited regions, methylamine (MeA) can be demethylated to acquire nitrogen (Karl et al., 2008; Repeta et al., 2016; Wang et al., 2021). The reductive demethylation of MPn and MeA produces methane as a reaction byproduct, suggesting that these alternative nutrient acquisition methods by surface ocean microbes may be responsible for aerobic methane production (Sosa et al., 2019; Wang et al., 2021).

Cyanobacteria can use aerobic methanogenic pathways under nutrient limited conditions (Arx et al., 2023). Cyanobacteria are ubiquitous in almost every environment. These photosynthetic bacteria have persisted for billions of years and helped shape Earth's early atmosphere during the Great Oxidation Event (Bižić et al., 2020). Most oxic methane research has focused on pelagic species of cyanobacteria, however, cyanobacteria also occur in microbial mats.

Microbial mats form in a range of environments, some of them extreme, such as hypersaline sediments, geothermal hot springs, hydrothermal vents, and tidal wetlands (Armitage et al., 2012). In intertidal environments, microbial mats are composed of vertically segregated layers of bacteria and diatoms. These microbes assemble based on millimeter-scale biogeochemical gradients, light intensity, and redox potential (Armitage et al., 2012). The uppermost layers of these mats are often dominated by oxygenic photosynthetic cyanobacteria, and these mats occur in salt marsh systems around the world (Armitage et al., 2012).

Microbial mats are well documented in coastal regions (Cardoso et al., 2019). Mats are extremely abundant in tropical and subtropical intertidal wetlands, such as in mangrove and salt

marsh systems, but they can also be found in temperate marshes as well as Arctic shorelines and ice shelves (Lee and Joye, 2006; Armitage et al., 2012; Varin et al., 2010). In temperate regions, mats are dominant in the summer months and dormant during the cooler seasons, whereas in subtropical and tropical regions, mats are present year-round (Cardoso et al., 2019). The development of mats in coastal environments is dependent on the extreme physiochemical conditions that impact microbial community composition, e.g. salinity levels, sediment grain size, light availability, erosion rates, grazing stress, and water table fluctuation (Stal et al., 1985; Carreira et al., 2015; Cardoso et al., 2019). Microbial mats are able to withstand steep biogeochemical gradients that change over short timescales as a result of daily variations in tides, nutrient availability, and temperature (Cardoso et al., 2019). The high diversity of microbial mat communities allows the mats to respond to acute changes in environmental parameters (Cardoso et al., 2019; Stal, 2001).

Cyanobacteria are usually the first microorganism to initiate microbial mat formation in low nutrient coastal wetlands (Stal et al., 1985; Stal, 2001). They provide structure and stability, thereby serving as a habitat for other microbes to colonize (Stal et al., 1985; Cardoso et al., 2019). Once the mat is formed, cyanobacteria are capable of scavenging nutrients from coastal waters and can provide essential nutrients to the other microorganisms in the mat (Varin et al., 2010). However, cyanobacteria are limited by phosphorus deficient conditions, which can occur in oligotrophic intertidal areas (Stal, 2001).

Wetlands are the largest terrestrial source of methane (Tiwari et al., 2019). Coastal marshes store large amounts of carbon and methane in sediments and have shifting nutrient gradients (Capooci et al., 2023; Drake et al., 2015). Nutrient loading in intertidal wetlands is dependent upon oceanic inputs that are regulated by seasonal and tidal patterns (Drake et al., 2015). It is well established that marshes in coastal areas are nitrogen limited, but they can also be co-limited by phosphorus, especially in young marsh systems (Sundareshwar et al., 2003; Van Wijnen & Bakker, 1999). Coastal plant communities are most often limited by nitrogen

3

availability, whereas marsh sediment bacterial communities are limited by phosphorus availability (Sundareshwar et al., 2003). This nutrient limitation has implications for carbon fixation and turnover within marsh sediments, as well as implications for bacterial aerobic methanogenesis in coastal wetlands (Van Wijnen & Bakker, 1999).

Salt marsh systems are ideal environments for microbial mat cyanobacteria to carry out aerobic methanogenesis. Nutrient dynamics and spatio-temporal patterns in coastal systems vary depending on geographical location, which impacts microbial mat community composition and areas where aerobic methanogenesis could occur (Cardoso et al., 2019). Daily tidal cycles, seasonal fluctuations, and clay accretion through marsh succession can cause nitrogen and phosphorus deplete conditions in intertidal wetlands and the surrounding waters (Van Wijnen & Bakker, 1999). In temperate salt marshes, braided tidal creeks and dense patches of the marsh grass *Spartina* reduce benthic-surface light availability, thus limiting mat formation to sandy sediments without vegetation (Armitage et al., 2012). Higher phosphorus concentrations may also impact aerobic methanogenesis in temperate marshes, as phosphorus presence should repress methane formation (Sosa et al., 2019).

Dissimilarly, subtropical salt marshes and tropical mangrove systems are chronically phosphorus limited, indicating that aerobic methanogenesis may be a viable pathway in these warmer areas (Sosa et al., 2019). These persistently low nutrient intertidal systems promote the growth of microbial mats through the presence of unvegetated hypersaline salt pans within marshes and the presence of dwarf mangrove forests within tropical wetlands, leading to high benthic light availability in both environments (Zhang et al., 2019; Lee and Joye, 2006). Nutrient limitation and favorable conditions in these coastal areas can therefore impact the location and microbial growth of salt marsh mats, causing mat cyanobacteria to potentially use aerobic methanogenic pathways to acquire essential nutrients and produce methane as a reaction byproduct (Wong et al., 2018). However, there is still uncertainty surrounding controls of coastal wetland methane emissions and no studies have assessed whether cyanobacteria-mediated

4

aerobic methane production occurs there (Capooci et al., 2023). This understudied process in salt marsh systems has implications for coastal methane dynamics and the global methane budget.

The aim of this work is to provide insight into the potential for aerobic methane production by cyanobacteria in salt marsh systems. To address whether coastal wetland cyanobacteria in microbial mats produce methane under nutrient limited conditions, the second chapter addresses how cyanobacteria use alternative aerobic methanogenesis pathways. The third chapter addresses whether benthic cyanobacteria have the metabolic genes necessary for aerobic methanogenesis using MPn under nutrient limitation. Understanding how methane is produced aerobically is key to understanding global methane cycling and climate change.

References:

Armitage, D. W., Gallagher, K. L., Youngblut, N. D., Buckley, D. H. & Zinder, S. H. (2012). Millimeter-scale patterns of phylogenetic and trait diversity in a salt marsh microbial mat. *Frontiers in Microbiology*, *3*, 293. https://doi.org/10.3389/fmicb.2012.00293

Arx, J. N. von, Kidane, A. T., Philippi, M., Mohr, W., Lavik, G., Schorn, S., Kuypers, M. M. M. & Milucka, J. (2023). Methylphosphonate-driven methane formation and its link to primary production in the oligotrophic North Atlantic. *Nature Communications*, *14*(1), 6529. https://doi.org/10.1038/s41467-023-42304-4

Bastviken, D., Tranvik, L. J., Downing, J. A., Crill, P. M. & Enrich-Prast, A. (2011). Freshwater methane emissions offset the continental carbon sink. *Science*, *331*(6013), 50–50. https://doi.org/10.1126/science.1196808

Bižić, M., Klintzsch, T., Ionescu, D., Hindiyeh, M. Y., Günthel, M., Muro-Pastor, A. M., Eckert, W., Urich, T., Keppler, F. & Grossart, H.-P. (2020). Aquatic and terrestrial cyanobacteria produce methane. *Science Advances*, *6*(3), eaax5343. https://doi.org/10.1126/sciadv.aax5343

Capooci, M., Seyfferth, A. L., Tobias, C., Wozniak, A. S., Hedgpeth, A., Bowen, M., … Vargas, R. (2023). High methane concentrations in tidal salt marsh soils: Where does the methane go? *Global Change Biology*, *30*(1), e17050. https://doi.org/10.1111/gcb.17050

Cardoso, D. C., Cretoiu, M. S., Stal, L. J. & Bolhuis, H. (2019). Seasonal development of a coastal microbial mat. *Scientific Reports*, *9*(1), 9035. https://doi.org/10.1038/s41598-019-45490-8

Carreira, C., Piel, T., Staal, M., Stuut, J.-B. W., Middelboe, M. & Brussaard, C. P. D. (2015). Microscale spatial distributions of microbes and viruses in intertidal photosynthetic microbial mats. *SpringerPlus*, *4*(1), 239. https://doi.org/10.1186/s40064-015-0977-8

Damm, E., Helmke, E., Thoms, S., Schauer, U., Nöthig, E., Bakker, K. & Kiene, R. P. (2010). Methane production in aerobic oligotrophic surface water in the central Arctic Ocean. *Biogeosciences*, *7*(3), 1099–1108. https://doi.org/10.5194/bg-7-1099-2010

Drake, K., Halifax, H., Adamowicz, S. C. & Craft, C. (2015). Carbon sequestration in tidal salt marshes of the northeast United States. *Environmental Management*, *56*(4), 998–1008. https://doi.org/10.1007/s00267-015-0568-z

Holmes, C. D., Prather, M. J., Søvde, O. A. & Myhre, G. (2013). Future methane, hydroxyl, and their uncertainties: key climate and emission parameters for future predictions. *Atmospheric Chemistry and Physics*, *13*(1), 285–302. https://doi.org/10.5194/acp-13-285-2013

Joye, S. B. (2020). The geology and biogeochemistry of hydrocarbon seeps. Annual Review of Earth and Planetary Sciences 48(1): 205–231. doi:10.1146/annurev-earth-063016-020052

Karl, D. M., Beversdorf, L., Björkman, K. M., Church, M. J., Martinez, A. & Delong, E. F. (2008). Aerobic production of methane in the sea. *Nature Geoscience*, *1*(7), 473–478. https://doi.org/10.1038/ngeo234

Lamontagne, R. A., Swinnerton, J. W., Linnenbom, V. J. & Smith, W. D. (1973). Methane concentrations in various marine environments. *Journal of Geophysical Research*, *78*(24), 5317–5324. https://doi.org/10.1029/jc078i024p05317

Lashof, D., Ahuja, D. (1990). Relative contributions of greenhouse gas emissions to global warming. Nature, 344, 529–531. https://doi.org/10.1038/344529a0

Lee, R. & Joye, S. (2006). Seasonal patterns of nitrogen fixation and denitrification in oceanic mangrove habitats. *Marine Ecology Progress Series*, *307*, 127–141. https://doi.org/10.3354/meps307127

Repeta, D. J., Ferrón, S., Sosa, O. A., Johnson, C. G., Repeta, L. D., Acker, M., DeLong, E. F. & Karl, D. M. (2016). Marine methane paradox explained by bacterial degradation of dissolved organic matter. Nature Geoscience, 9(12), 884–887. https://doi.org/10.1038/ngeo2837

Saunois, M., Stavert, A. R., Poulter, B., Bousquet, P., Canadell, J. G., Jackson, R. B., Raymond, P. A., … Zhuang, Q. (2020). The global methane budget 2000–2017. Earth System Science Data, 12(3), 1561–1623. https://doi.org/10.5194/essd-12-1561-2020

Sosa, O. A., Repeta, D. J., DeLong, E. F., Ashkezari, M. D. & Karl, D. M. (2019). Phosphate-limited ocean regions select for bacterial populations enriched in the carbon–phosphorus lyase pathway for phosphonate degradation. Environmental Microbiology, 21(7), 2402–2414. https://doi.org/10.1111/1462-2920.14628

Stal, L. J., Gemerden, H. van & Krumbein, W. E. (1985). Structure and development of a benthic marine microbial mat. *FEMS Microbiology Ecology*, *1*(2), 111–125. https://doi.org/10.1111/j.1574-6968.1985.tb01138.x

Stal, L. J. (2001). Coastal microbial mats: the physiology of a small-scale ecosystem. *South African Journal of Botany*, *67*, 399–410.

Sundareshwar, P. V., Morris, J. T., Koepfler, E. K. & Fornwalt, B. (2003). Phosphorus limitation of coastal ecosystem processes. *Science*, *299*(5606), 563–565. https://doi.org/10.1126/science.1079100

Tiwari, S., Singh, C., Singh, J. S. (2020). Wetlands: A Major Natural Source Responsible for Methane Emission. Restoration of Wetland Ecosystem: A Trajectory Towards a Sustainable Environment. Springer. https://doi.org/10.1007/978-981-13-7665-8_5

Van Wijnen, H. J. & Bakker, J. P. (1999). Nitrogen and phosphorus limitation in a coastal barrier salt marsh: the implications for vegetation succession. *Journal of Ecology*, *87*(2), 265–272. https://doi.org/10.1046/j.1365-2745.1999.00349.x

Varin, T., Lovejoy, C., Jungblut, A. D., Vincent, W. F. & Corbeil, J. (2010). Metagenomic profiling of Arctic microbial mat communities as nutrient scavenging and recycling systems. *Limnology and Oceanography*, *55*(5), 1901–1911. https://doi.org/10.4319/lo.2010.55.5.1901

Wang, Q., Alowaifeer, A., Kerner, P., Balasubramanian, N., Patterson, A., Christian, W., Tarver, A., Dore, J. E., Hatzenpichler, R., Bothner, B. & McDermott, T. R. (2021). Aerobic bacterial methane synthesis. Proceedings of the National Academy of Sciences, 118(27), e2019229118. https://doi.org/10.1073/pnas.2019229118

Wong, H. L., White, R. A., Visscher, P. T., Charlesworth, J. C., Vázquez-Campos, X. & Burns, B. P. (2018). Disentangling the drivers of functional complexity at the metagenomic level in Shark Bay microbial mat microbiomes. *The ISME Journal*, *12*(11), 2619–2639. https://doi.org/10.1038/s41396-018-0208-8

Zhang, C., Mishra, D. R. & Pennings, S. C. (2019). Mapping salt marsh soil properties using imaging spectroscopy. *ISPRS Journal of Photogrammetry and Remote Sensing*, *148*, 221–234. https://doi.org/10.1016/j.isprsjprs.2019.01.006

CHAPTER 2

AEROBIC METHANOGENESIS IN MICROBIAL MATS

Introduction:

Phosphorus and nitrogen are essential macronutrients for marine microorganisms. However, oligotrophic waters in the Atlantic and Pacific are typically nutrient-limited (Moore et al., 2013). These waters are characterized by low phosphorus, while the Atlantic is also co-limited by nitrogen (Moore et al., 2013; Sosa et al., 2019). Under phosphorus and nitrogen deficiency, microbes use alternative pathways to acquire nutrients from other organic compounds (Sosa et al., 2019; Kamat et al., 2011)

Phosphonates are one of the largest classes of compounds in oligotrophic regions that contain phosphorus. Methylphosphonate (MPn) is a low-molecular-weight (LWM) phosphonate that is abundant in semi-labile dissolved organic matter (Repeta et al., 2016). Pelagic microbes such as cyanobacteria are capable of breaking the characteristic C-P bond in MPn using specialized enzymes; this action allows them to acquire inorganic phosphorus from phosphonates under phosphorus limited conditions. The reductive demethylation pathway of MPn breakdown produces methane as a reaction byproduct and may be responsible for the oceanic methane paradox (Sosa et al., 2019). The MPn pathway has been well defined and extensively studied in the Pacific, Atlantic, and lake systems (Karl et al., 2008; Repeta et al., 2016, Arx et al., 2023; Bižić-Ionescu et al., 2019).

Under nitrogen limited conditions, methylamine metabolism by microbes can produce methane by utilizing a different demethylation pathway (Bižić-Ionescu et al., 2019; Wang et al., 2021). Methylamine (MeA) is a LMW carbon compound that is the product of organic matter decomposition; it is also the breakdown product of glycine betaine, an osmolyte used by microbes and plants. Methylamine is used as a substrate for a well-described anaerobic methylotrophic methanogenesis pathway (Zhuang et al., 2018). However, the contribution of the

reductive demethylation MeA pathway to aerobic methanogenesis is not as well constrained as the MPn pathway (Wang et al., 2021).

Aerobic methane production studies have not been conducted in salt marsh systems. Marshes are dynamic ecosystems but can be nutrient limited depending on location and the tides. Several studies have shown that cyanobacteria in microbial mats use the MPn pathway, but these mat cultures were isolated from geothermal hot springs or from stromatolites (Gomez-Garcia et al., 2011; Wong et al., 2018). Additionally, MeA use by cyanobacteria has only been shown in a lake system (Wang et al., 2021). This chapter will explore potential aerobic MPn and MeA use by cyanobacteria in salt marsh microbial mats to provide insight into coastal methane dynamics.

<u>Methods:</u>

Description of Study Site

Microbial mat samples were collected from a subtropical barrier island along the coast of Georgia, USA. The sampling sites on this island were located in salt marsh areas that were ideal for microbial mat growth within the high marsh. The primary sampling site was located on Skidaway Island near the Skidaway Institute of Oceanography. This coastal research institute was founded in 1968 and merged with the University of Georgia in 2013. The Normalized Difference Vegetation Index (NDVI) was calculated for the Skidaway area using spectrometric data from NASA's Landsat 8 Earth Observation Satellite to identify areas of the high marsh (Supplementary Figure S1). An expansive high marsh area near an institute-owned dock was identified and sampled for microbial mats on August 24th, 2023 (31.963°N, 81.014°W).

Mat Collection

Mat samples were collected from a high marsh area on Skidaway Island. The high marsh zone was inundated infrequently during high tides, but the high water table kept the

sediments and mats saturated. Pickleweed (*Salicornia spp.*) was used as an indicator of high salinity areas within the marsh owing to its salt tolerance, which was helpful for identifying areas where microbial mats may be present.

Mats were identified based on characteristic blue green patches atop marsh sediment that occasionally had bubbles created by oxygen production. A sterile scalpel was used to cut out 14 in x 11 in sections of mat from the marsh that included about 2 cm of underlying sediment. Mats were transferred to acid washed HDPE containers using sterilized HDPE cutting boards so as to not directly touch the mat surface. Overlying water was then collected from the nearest tidal creek using either 10 L plastic cubitainers or 1 L PETG bottles.

The mat containers were left uncovered overnight before being closed during transport (approximately 4 hours). Mat samples were then uncovered and placed outside in semi-direct sunlight (~1100 μ Einsteins) for five days to re-acclimate to the natural day/night circadian cycle. During this time, samples were kept moist using 500 mL of overlying site specific water per day.

Mat Incubation

A time series incubation experiment was run using the Skidaway mat samples. Three controls (seawater, unamended mat, and killed) and four amendments (+MPn, +MeA, +MPn+NH_4, and +MeA+PO_4) were implemented. Four replicates were included for each control and treatment. Samples were incubated under either a natural light/dark cycle (light) or strictly dark conditions for a total sample size of 56 vials (n = 28 per light treatment).

Eight 1 cm^3 cores were taken from the mat using an autoclaved 5 mL cut end plastic syringe. Cores were wrapped in aluminum foil and autoclaved to serve as killed controls. These killed cores were rinsed with 10 mL of filtered site-specific seawater four times to remove excess dissolved organic carbon generated during autoclaving.

Seawater controls contained no mat, thus eight 20 mL serum vials were filled with 10 mL of filtered site-specific seawater before being stoppered and crimp sealed. 48 additional cores

were removed from the mat to be used for the unamended mat control, +MPn, +MeA, +MPn+NH_4, and +MeA+PO_4 treatments. Killed control samples and amended treatments were placed into 20 mL serum vials and 10 mL of filtered site-specific seawater was added.

1 mM methanephosphonic acid, 1 mM trimethylamine hydrochloride, 1 mM ammonium chloride, and 100 µM potassium phosphate were used for the amendments. 100 µL of each amendment solution was added to the respective treatment vial. Final incubation concentrations of MPn, MeA, and NH_4 were 10 µM and the final concentration of PO_4 was 1 µM.

All vials were stoppered and crimp sealed. 28 vials (four replicates for each of the seven treatments) were wrapped in aluminum foil to serve as the dark-only treatment. All vials were placed under a Sun Systems 5K volt grow light (~500 µ Einsteins) and incubated on a light (6 am - 6 pm) / dark (6 pm - 6 am) cycle to mimic natural diel cycles. Light could not penetrate the aluminum foil wrapped dark-only treatment vials, so they were maintained under the grow light along with the light treatments to ensure a consistent temperature across all samples.

Headspace methane was immediately pulled from all samples for the time 0 incubation point. This was done by removing 1 mL of headspace from each vial using a 5 mL plastic syringe and replacing it with 1 mL of UHP nitrogen gas (UN1066) to ensure a stable pressure. Headspace samples were directly injected into a GC-FID (SRI, 8610C) with a 50 m HP-AL/S column. The injection/detection temperature was 250°C and the column was set at 40°C with a run time of 2.5 minutes. Samples were run in tandem with aqueous methane standards. Methane peaks were recorded for all standards and samples run on the GC.

Once samples were run on the GC, they were placed back under the grow light. Headspace methane was measured in the same process at 12, 24, 36, 48, 72, 96, 120, and 144 hours from the start of the incubation. This was done to measure methane production at 6 am and 6 pm timepoints that reflected natural sunrise and sunset times.

Post Incubation Geochemical Analysis

After headspace methane samples were run at the 144-hour time point, all vials were de-crimped and opened. A 10 mL plastic syringe was used to remove any liquid within each vial to be used for post incubation geochemical analysis. Incubation water from replicates was pooled together and filtered using a 0.2 µm Target filter into 60 mL HDPE bottles. Target filters were rinsed with 10 mL of MQ, followed by 2 mL of sample prior to filtration.

2.5 mL of filtered sample was subsampled into 15 mL Falcon tubes and preserved with 100 µL phenol to be analyzed using the ammonium colorimetric method described by Solorzano (1969). Samples were stored at 20°C.

Samples were analyzed for nitrite (NO_2^-), NO_x^- (sum of nitrate and nitrite), phosphate (PO_4^{3-}), total dissolved phosphate (TDP), total dissolved nitrogen (TDN), and dissolved organic carbon (DOC) within 3 weeks of the end of the incubation.

Phosphate concentrations were measured with the molybdate blue colorimetric method described by Strickland and Parsons (1972). TDP was analyzed colorimetrically as PO_4^{3-} after samples were combusted and acid hydrolyzed (Solorzano and Sharp, 1980). Nitrite concentrations were measured using a colorimetric method described by Bendschneider and Robinson (1952) as reproduced by Parsons, Maita, and Lalli (1984).

DOC and TDN were analyzed on a Shimadzu TOC-Vcph. Samples were run in tandem with potassium hydrogen phthalate standards and glycine standards, respectively. NO_x^- concentrations were measured by vanadium (III) reduction and a chemiluminescent nitric oxide reaction using an Antek 7050 nitric oxide detector (Braman and Hendrix, 1983). Detection limits for all geochemical analyses were noted (Supplementary Table S1).

Statistical Analysis

Average methane concentrations and rates of production were calculated for each time point. Methane concentration data were background-corrected using the seawater control.

Rates were calculated as the methane concentration (nmol) per area of mat core (m^2) per day. 95% confidence intervals on the mean were generated for every treatment at each time point using the t.test() function of R (v. 4.4.1, R Core Team 2024). Figures were also generated with R. Differences in means are considered statistically significant if the confidence intervals do not overlap, but they are considered statistically indistinguishable if their confidence intervals do overlap.

Results and Discussions:

Post Incubation Geochemical Characteristics

Light and dark NO_2^-, NO_X^-, PO_4^{3-}, TDP, and DOC concentrations follow relatively similar trends across controls and amended samples (Table 1). The NO_X^-, PO_4^{3-}, and TDP control and amended concentrations are lower than the seawater controls, except for the killed controls which are much higher. The NO_2^- and DOC controls and amended concentrations are higher than the seawater controls (Table 1).

For light NH_4 values, the unamended mat control and MeA amendment had lower concentrations than the seawater control, whereas the MPn+N amendment had higher concentrations. The dark NH_4 concentrations were all higher than the seawater control samples (Table 1).

The TDN values also have different trends between light and dark (Table 1). All light treatments have higher concentrations of TDN than the seawater control, with the killed control being the highest. The dark treatments also have higher TDN concentrations compared with the seawater control, but the unamended mat control and MPn amendment have the highest concentrations among the dark samples.

Table 1: Geochemical measurements of mat incubation water post incubation. Samples were analyzed for ammonium (NH_4), nitrite (NO_2^-), the sum of nitrate and nitrite (NO_x^-), phosphate (PO_4^{3-}), total dissolved phosphate (TDP), total dissolved nitrogen (TDN), and dissolved organic carbon (DOC).

Sample	NH_4 (µM)	NO_2^- (µM)	NO_x^- (µM)	PO_4^{3-} (µM)	TDP (µM)	TDN (µM)	DOC (µM)
SW-L	1.18	0.24	1.06	3.79	6.38	42	875
M-L	0.59	0.37	0.41	0.63	0.09	67	965
K-L	209	0.12	0.47	31	49	870	6381
MP-L	1.11	0.35	0.32	0.11	1.08	70	1034
MA-L	0.32	0.33	0.43	0.53	0.15	75	1077
MP+N-L	3.88	0.35	0.34	0.58	2.34	89	1279
MA+P-L	0.39	0.35	0.39	0.63	0.22	73	1124
SW-D	29	0.17	1.39	6.95	8.96	71	555
M-D	358	0.24	0.29	0.47	0.31	825	810
K-D	190	0.09	0.49	17	32	653	3744
MP-D	343	0.20	0.21	0.11	1.54	865	1075
MA-D	318	0.22	0.40	0.58	0.38	712	819
MP+N-D	214	0.35	0.59	1.89	10	431	910
MA+P-D	232	0.35	0.46	0.31	0.28	479	929

Light Treatment Potential Methanogenesis Rates

Light treatment samples indicate methane production from MPn+NH_4 and MPn amendments, but it is unknown whether this production was from aerobic or anaerobic processes (Figures 1 and 2). All of the methane concentrations for the light treatment samples are very low, and most concentrations are below the detection limit. Any methane concentration below the detection limit is plotted as a zero. Samples that produced methane have concentrations that are above the detection limit, meaning methane concentrations are greater than the controls by more than three standard deviations.

MPn+NH_4 and MPn amended samples have similar methane concentration values over the duration of the incubation. Both treatments have concentrations that are significantly different (i.e. the confidence intervals on their means do not overlap) for the last three time points, but the two treatments cannot be distinguished from one another at any time point or from the controls at the 48- and 72-hour time points (Figure 1). MPn+NH_4 and MPn amended

samples have quantifiable methane concentrations compared with the other amendments. Concentrations reach a maximum of 2.5 ± 2.1 nmol (95% C.I.) and 2.1 ± 0.9 nmol (95% C.I.), respectively, at 144 hours (Figure 1). MeA samples produced very low methane concentrations, but these are below the detection limit and therefore not quantifiable.

The timing of methane production is the same for the $MPn+NH_4$ and MPn amendments (Figure 1). Methane concentrations began to increase at the 48-hour time point for the $MPn+NH_4$ and MPn amended samples. Concentrations continue to increase over the duration of the incubation before reaching maximum concentrations at the 144-hour time point. All other amendments and controls have concentrations that are below the detection limit.

$MPn+NH_4$ and MPn amended samples have the highest rates of production, but they are not distinguishable from each other (i.e. the confidence intervals on their means overlap) and, with one exception, are not distinguishable from the controls (Figure 2). The $MPn+NH_4$ and MPn treatments have nearly identical initial rates at the 48-hour time point. However, the rates of these two amendments differ after reaching a maxima at 48 hours. MPn decreases at a relatively consistent rate over the remainder of the incubation. $MPn+NH_4$ decreases to a minimum at the 72-hour time point, but production rates increase after that. Rates reach an overall maximum rate of 93.9 ± 63.4 $nmol/m^2/day$ (95% C.I.) at 96 hours. This second maximum is the only rate value that is significantly different from the controls. Rates drop off at the end of the incubation. All other amendments and controls have rates that are below the detection limit.
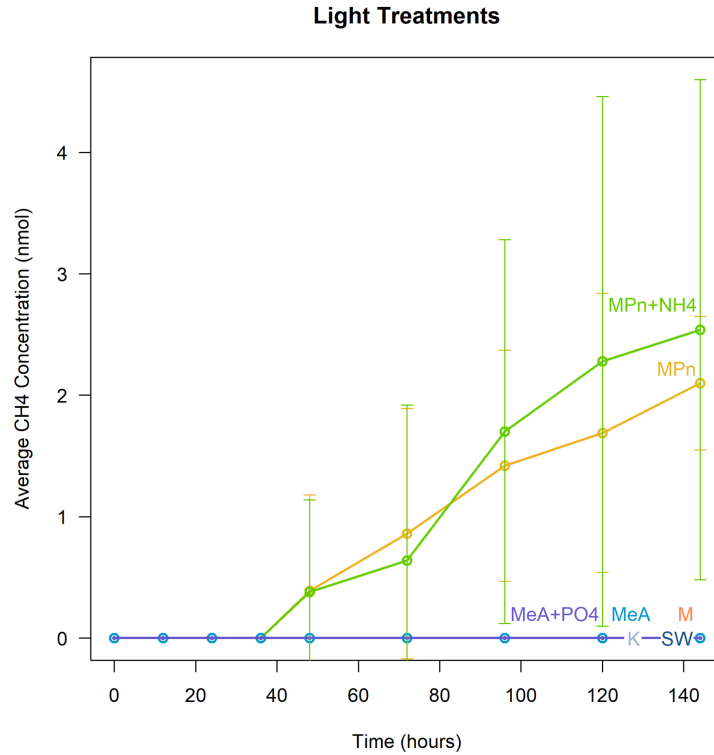
Figure 1: Average CH_4 concentrations (nmol) for all light treatments (n=4 per treatment) measured over the duration of the incubation (144 hours). Bars are 95% confidence intervals on the mean.

Figure 2: Average CH_4 rates (nmol / m^2 / day) for all light treatments (n=4 per treatment) calculated from measured CH_4 concentrations and the area of the mat cores. Rates of production are values above zero, whereas rates of consumption are values below zero. Bars are 95% confidence intervals on the mean.

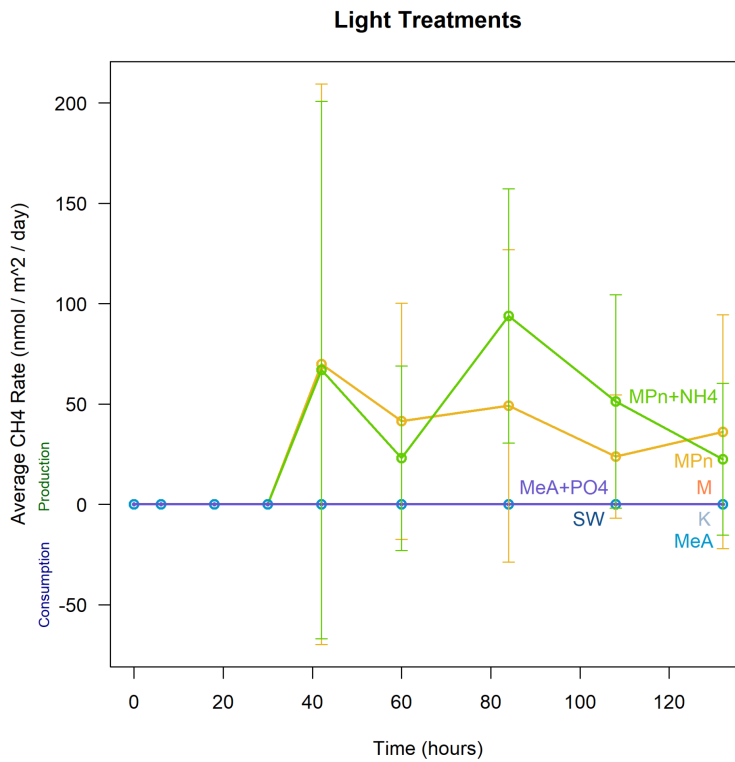*Dark Treatment Potential Methanogenesis Rates*

       Dark treatment samples show methane production from the unamended mat treatment and all amended samples, mainly from the MeA and MPn amendments (Figures 3 and 4). Although methane concentrations for the dark treatment samples are also low, more of the values are above the detection limit than concentrations from the light treatment samples. Values that are below the detection limit are plotted as zero.

       MeA amended samples have the highest methane concentrations of the incubation across all treatment types (Figure 3). This treatment has concentrations that are significantly different from the seawater and kill controls, but can not be distinguished from the unamended mat treatment or the other amendments at most time points. MeA concentrations reach a maximum of 96.1 ± 28.1 nmol (95% C.I.) at 144 hours. The MPn, MeA+PO_4, and MPn+NH_4 amendments have similar methane concentrations over the course of the incubation, reaching maximum values of 46.7 ± 41.8 nmol (95% C.I.), 27.0 ± 13.1 nmol (95% C.I.), and 22.9 ± 23.7 nmol (95% C.I.) at 144 hours, respectively. These treatments are distinguishable from the seawater and kill controls, but not from each other. The unamended mat control produces methane, reaching a maximum concentration of 32.7 ± 25.9 nmol (95% C.I.) at the 144-hour time point. This control is distinguishable from the seawater and kill controls, as they have concentrations below the detection limit.

       The timing of methane production is the same for the unamended mat treatment and all of the amendments (Figure 3). Methane concentrations begin to increase significantly at the 72-hour time point. The MeA, MeA+PO_4, and MPn+NH_4 amendments have concentrations of 1.8 ± 2.2 nmol (95% C.I.), 3.5 ± 4.4 nmol (95% C.I.), and 0.64 ± 2.0 nmol (95% C.I.) at 72 hours, respectively. The unamended mat control has the highest 72-hour concentration of 4.1 ± 8.9 nmol (95% C.I.). The MeA+PO_4 amendment and unamended mat treatment have higher concentrations at 72 hours than the maximum methane concentrations for the light treatment samples at any time point. However, none of the dark concentrations at 72 hours are

18

distinguishable from each other or from the seawater and kill controls. Methane concentrations continue to increase over the remainder of the incubation for all treatments except the seawater and kill controls, which are below the detection limit. Maximum concentrations are recorded at the 144-hour time point for the unamended mat control and all amendments.

Methane rates begin to increase around 72 hours for all samples except the seawater and kill controls, but the timing of when rates decrease varies among amendments (Figure 4). MeA, MeA+PO_4, and MPn+NH_4 amendments reach their maximum rate before the last time point of the incubation. MeA has the highest recorded rate of 4,188 ± 1,462 nmol/m^2/day (95% C.I.) at 120 hours, which is significantly different from all amendments and controls. MPn+NH_4 also reach a maximum rate at 120 hours of 948 ± 798 nmol/m^2/day (95% C.I.). Both the MeA and MPn+NH_4 rates decrease at 144 hours to 3,008 ± 1,446 nmol/m^2/day (95% C.I.) and 252 ± 224 nmol/m^2/day (95% C.I.), respectively, with only MeA being distinguishable from the controls. MeA+PO_4 samples peak at the 96-hour time point (1,259 ± 869 nmol/m^2/day (95% C.I.)) before steadily decreasing to 120 ± 254 nmol/m^2/day (95% C.I.) by 144 hours. Neither of the MeA+PO_4 rate values at either time point are distinguishable from the other amendments.

The rates of methane production for the MPn amendment and the unamended mat control never decrease during the incubation (Figure 4). MPn amended samples have a maximum rate of 2,604 ± 2,256 nmol/m^2/day (95% C.I.) at 144 hours, although this rate is distinguishable from the controls but not from the amendments. The unamended mat treatment also reaches a maximum rate at 144 hours of 1,003 ± 1,041 nmol/m^2/day (95% C.I.), and this rate is similarly distinguishable from the controls but not from the other amendments.
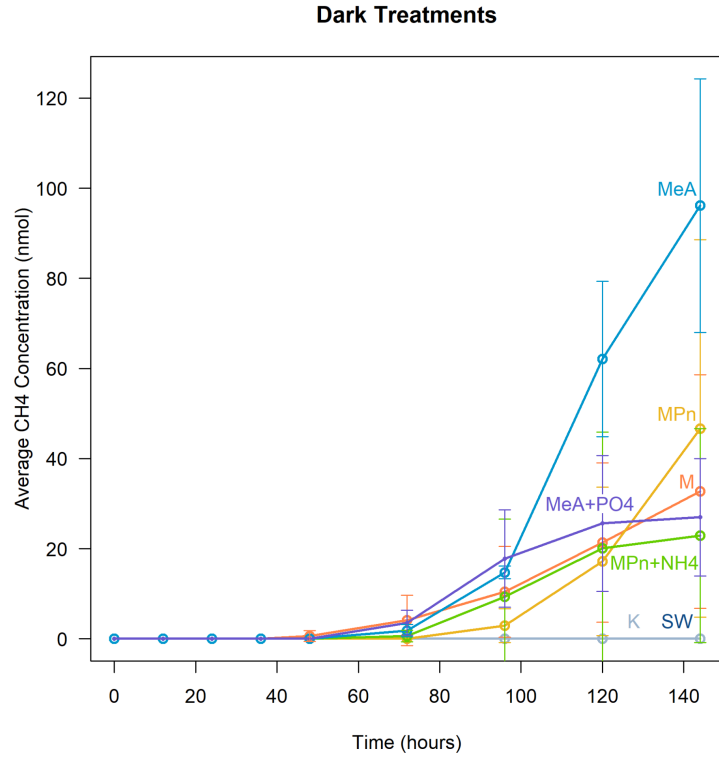
Figure 3: Average CH_4 concentrations (nmol) for all dark treatments (n=4 per treatment) measured over the duration of the incubation (144 hours). Bars are 95% confidence intervals on the mean.
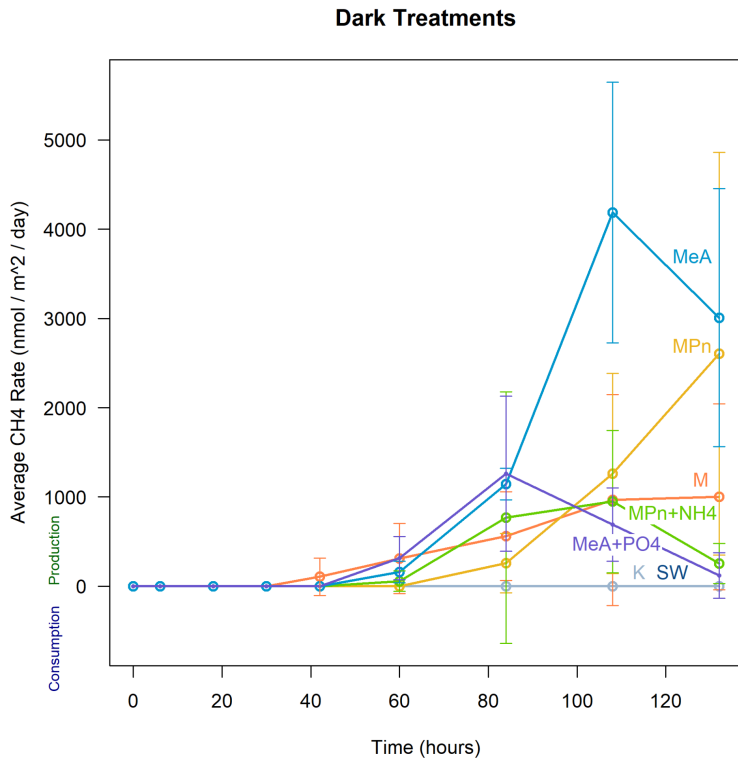
Figure 4: Average CH_4 rates (nmol / m^2 / day) for all dark treatments (n=4 per treatment) calculated from measured CH_4 concentrations and the area of the mat cores. Rates of production are values above zero, whereas rates of consumption are values below zero. Bars are 95% confidence intervals on the mean.

Conclusions:

Trends in Light Methanogenesis

Methane production varies among amended samples and light treatment types. The light treatment MPn+NH$_4$ and MPn methane concentrations are low (Figures 1 and 2). Although the concentrations of these two amendments are similar, the rates of production differ over the course of the incubation. Differences in light-driven oxic methane production among amendments should be caused by nutrient availability and utilization by microbial mat microbes. However, as it is unknown if or when the vials went anoxic, no conclusions can be made about whether aerobic processes occurred.

The MPn+NH$_4$ amendments are phosphorus limited, as the system shifted to phosphorus limitation because of NH$_4$ addition. Cyanobacteria in the microbial mats therefore should have been able to use the reductive demethylation MPn pathway to acquire phosphorus, producing methane as a byproduct. However, this process occurs under phosphorus depleted, oxic conditions. The final PO$_4^{3-}$ concentration of the MPn+NH$_4$ amendment was 0.58 µM, indicating that complete phosphorus drawdown did not occur in that treatment (Table 1). Initial MPn+NH$_4$ concentrations and rates could potentially be caused by aerobic methanogenesis if the vials were oxic, but incomplete phosphorus drawdown suggests that the reductive demethylation of MPn likely did not occur in those samples.

High concentrations of phosphorus should repress methane formation, as microbes should not need to demethylate methylphosphonate to acquire phosphorus since it is present in abundance. However, samples amended with MPn produce methane even though N:P ratios calculated from the post incubation geochemical analyses indicate that the light treatment vials are phosphorus-replete. Although it cannot be concluded whether this methane production originated from aerobic or anaerobic pathways, methane should not have been produced aerobically if the vials were oxic. Arx et al. (2023) report that methylphosphonate utilization by pelagic cyanobacteria in oxic settings can persist even under phosphorus-replete conditions.

21

This demonstrates that microbial mat cyanobacteria can potentially undergo aerobic methanogenesis in intertidal systems that are not phosphorus limited. Some cyanobacteria species are also able to constitutively express the MPn pathway regardless of phosphorus limitation, which could be another explanation as to why methane production occurred.

MeA samples produce methane concentrations that are below the detection limit. The reductive demethylation of MeA is a novel pathway that has yet to be well constrained. Although MeA sample concentrations and rates could not be quantified, some studies indicate that methylamine methane production through oxic methanogenesis pathways is viable in cyanobacteria (Wang et al., 2021).

Trends in Dark Anaerobic Methanogenesis

Methane concentrations are higher in the dark treatment samples than the light treatment concentrations, and they have different production trends. Cyanobacteria are photosynthetic organisms that use nutrients to thrive in almost every environment. This means there should not have been oxic methane production from the dark samples as there was no sunlight available for photosynthesis. However, all samples except the seawater and kill controls begin to produce methane around the 72-hour time point (Figures 3 and 4). It can therefore be assumed that the dark vials went anoxic and anaerobic methanogenesis began to occur as there was quantifiable methane production without the presence of sunlight.

The seawater and kill controls did not produce methane, as any microbes within the cores are killed during the autoclaving process. This indicates that other microorganisms within the microbial mat or sediment are present and capable of mediating anaerobic methanogenesis, as methane is produced in the unamended mat control and all other amendments.

The MeA and MPn samples have the highest concentrations and rates of methane production, which are significantly different from the controls. Methylamine and methylphosphonate are methylated compounds that can be used as substrates in anaerobic

methylotrophic methanogenesis (Zhuang et al., 2018). This could explain why methane production is much higher in MeA and MPn samples than the other amendments. Methylated compounds are also present in the MeA+PO$_4$ and MPn+NH$_4$ samples, which could be why those treatments also saw methane formation.

Aerobic Methanogenesis Implications

Methane production from the dark treatment vials began to significantly increase around the 72-hour time point, indicating that the vials went anoxic and anaerobic methanogenesis was occurring (Figures 3 and 4). However, the exact timing of when the dark vials went anoxic is unknown. The 72-hour time point had dark average methane concentrations of 2.54 ± 4.4 nmol (95% C.I.) and dark average rates of 210 ± 347 nmol/m^2/day (95% C.I.), but time points before then have concentrations that are below the detection limit. These low concentrations at the earlier time points could result from the balance of methane production and methane oxidation. If the dark vials went anoxic near the start of the incubation from a lack of sunlight available for photosynthesis, methane production could have been matched by methane oxidation during the earlier time points as methanotrophs in the microbial mat consumed methane (Valentine & Reeburgh, 2000). However, the dark methane concentrations and rates of production began to increase significantly around the 72-hour time point. This could indicate the time point when rates of methane production overtook rates of methane oxidation, leading to quantifiable concentrations of methane over the remainder of the incubation.

Similarly to the dark treatments, it is unknown if or when the light treatment vials went anoxic as oxygen was not measured within the vials. However, it should be noted that microorganisms in the light treatment vials were able to use photosynthetic pathways and produced oxygen bubbles during the earlier time points of the incubation. Oxygen bubbles were present at the start of the incubation but slowly dwindled in size and number until they disappeared at the 72-hour time point. This indicates that the light treatment microbes were

capable of photosynthesis and theoretically able to use aerobic methanogenic pathways as oxygen was produced as a photosynthetic byproduct. However, it is unknown if or when the light treatment vials went anoxic and therefore it is not possible to determine whether the aerobic or anaerobic methanogenic pathway was responsible for light methane production.

Although it is not possible to conclude that methane was produced under oxic conditions during the incubation, this study has implications for the potential use of MPn and MeA by cyanobacteria in salt marsh microbial mats to produce methane through aerobic methanogenic pathways. Other microorganisms present within the microbial mat besides cyanobacteria may have produced methane. Without a photosynthesis inhibitor, it is not possible to conclude that cyanobacteria were solely responsible for methane production. However, this study is the first to investigate the potential for aerobic MPn and MeA methanogenesis by microbial mats in understudied salt marsh systems. In addition, observed findings indicate that nutrient dynamics in intertidal wetlands and nutrient utilization by cyanobacteria may play a critical role in coastal methane regulation.

References:

Arx, J. N. von, Kidane, A. T., Philippi, M., Mohr, W., Lavik, G., Schorn, S., Kuypers, M. M. M. &
    Milucka, J. (2023). Methylphosphonate-driven methane formation and its link to primary
    production in the oligotrophic North Atlantic. *Nature Communications*, *14*(1), 6529.
    https://doi.org/10.1038/s41467-023-42304-4

Bendschneider, K., Robinson, R.J. (1952). A new spectrophotometric method for the
    determination of nitrite in sea water. *University of Washington Oceanographic
    Laboratories*. http://hdl.handle.net/1773/15938

Bižić-Ionescu, M., Ionescu, D., Günthel, M., Tang, K. W. & Grossart, H.-P. (2019). *Biogenesis of
    Hydrocarbons*. 379–400. https://doi.org/10.1007/978-3-319-78108-2_10

Braman, R.S., Hendrix, S.A. (1989). Nanogram nitrite and nitrate determination in environmental
    and biological materials by vanadium (III) reduction with chemiluminescence detection.
    Analytical Chemistry, 61(24), 2715-2718. https://doi.org/10.1021/ac00199a007

Gomez-Garcia, M. R., Davison, M., Blain-Hartnung, M., Grossman, A. R. & Bhaya, D. (2011).
    Alternative pathways for phosphonate metabolism in thermophilic cyanobacteria from
    microbial mats. *The ISME Journal*, *5*(1), 141–149. https://doi.org/10.1038/ismej.2010.96

Kamat, S. S., Williams, H. J. & Raushel, F. M. (2011). Intermediates in the transformation of
    phosphonates to phosphate by bacteria. *Nature*, *480*(7378), 570–573.
    https://doi.org/10.1038/nature10622

Karl, D. M., Beversdorf, L., Björkman, K. M., Church, M. J., Martinez, A. & Delong, E. F. (2008).
    Aerobic production of methane in the sea. *Nature Geoscience*, *1*(7), 473–478.
    https://doi.org/10.1038/ngeo234

Moore, C. M., Mills, M. M., Arrigo, K. R., Berman-Frank, I., Bopp, L., Boyd, P. W., Galbraith, E.
    D., Geider, R. J., Guieu, C., Jaccard, S. L., Jickells, T. D., Roche, J. L., Lenton, T. M.,
    Mahowald, N. M., Marañón, E., Marinov, I., Moore, J. K., Nakatsuka, T., Oschlies, A., …
    Ulloa, O. (2013). Processes and patterns of oceanic nutrient limitation. *Nature
    Geoscience*, *6*(9), 701–710. https://doi.org/10.1038/ngeo1765

Parsons, T.R., Maita, T., Lalli, C.M. (1984). A manual of chemical and biological methods for
    seawater analysis. Oxford, UK, Pergamon, Press, 173. http://dx.doi.org/10.25607/OBP-
    1830

R Core Team. 2024. R: a language and environment for statistical computing. R Foundation for
    Statistical Computing, Vienna, Austria. https://www.R-project.org

Repeta, D. J., Ferrón, S., Sosa, O. A., Johnson, C. G., Repeta, L. D., Acker, M., DeLong, E. F. & Karl, D. M. (2016). Marine methane paradox explained by bacterial degradation of dissolved organic matter. *Nature Geoscience*, *9*(12), 884–887. https://doi.org/10.1038/ngeo2837

Solorzano, L. (1969). Determination of ammonia in natural waters by phenolhypochlorite method. *Limnology and Oceanography*, 9, 799-801. https://doi.org/10.4319/lo.1969.14.5.0799

Solorzano, L., Sharp, J.H. (1980). Determination of total dissolved phosphorus and particulate phosphorus in natural waters. *Limnology and Oceanography*, 25(4), 754-758. https://doi.org/10.4319/lo.1980.25.4.0754

Sosa, O. A., Repeta, D. J., DeLong, E. F., Ashkezari, M. D. & Karl, D. M. (2019). Phosphate-limited ocean regions select for bacterial populations enriched in the carbon–phosphorus lyase pathway for phosphonate degradation. *Environmental Microbiology*, *21*(7), 2402–2414. https://doi.org/10.1111/1462-2920.14628

Strickland, J. D. H. & Parsons, T. R. (1972). A Practical Handbook of Seawater Analysis. *Fisheries Research Board of Canada*. http://dx.doi.org/10.25607/OBP-1791

Valentine, D. L. & Reeburgh, W. S. (2000). New perspectives on anaerobic methane oxidation. *Environmental Microbiology*, *2*(5), 477–484. https://doi.org/10.1046/j.1462-2920.2000.00135.x

Wang, Q., Alowaifeer, A., Kerner, P., Balasubramanian, N., Patterson, A., Christian, W., Tarver, A., Dore, J. E., Hatzenpichler, R., Bothner, B. & McDermott, T. R. (2021). Aerobic bacterial methane synthesis. *Proceedings of the National Academy of Sciences*, *118*(27), e2019229118. https://doi.org/10.1073/pnas.2019229118

Wong, H. L., White, R. A., Visscher, P. T., Charlesworth, J. C., Vázquez-Campos, X. & Burns, B. P. (2018). Disentangling the drivers of functional complexity at the metagenomic level in Shark Bay microbial mat microbiomes. *The ISME Journal*, *12*(11), 2619–2639. https://doi.org/10.1038/s41396-018-0208-8

Zhuang, G., Peña-Montenegro, T. D., Montgomery, A., Hunter, K. S. & Joye, S. B. (2018). Microbial metabolism of methanol and methylamine in the Gulf of Mexico: insight into marine carbon and nitrogen cycling. *Environmental Microbiology*, *20*(12), 4543–4554. https://doi.org/10.1111/1462-2920.14406

CHAPTER 3

GENE MARKERS OF BENTHIC CYANOBACTERIA

Introduction:

Phosphorus is vital for the growth and metabolism of microorganisms, however, this essential molecule is limiting in most surface oceans (Duhamel et al., 2021). Vast regions in the subtropics and tropics are notably depleted in phosphorus, which can suppress marine productivity. In order to gain the essential nutrients they need, microbes can extract phosphorus from other organic compounds, such as phosphonates (Sosa et al., 2019).

Phosphonates are characterized by a stable carbon-phosphorus (C-P) bond (White and Metcalf, 2007). They make up a substantial part of the phosphorus pool and marine dissolved organic matter (Metcalf et al., 2012). Microbes have evolved specific enzymes to break the C-P bonds of phosphonates to acquire inorganic phosphorus under phosphorus limitation (Arx et al., 2023; Sosa et al., 2019).

C-P lyase is a multi-enzyme complex that is regulated by the Pho regulon and expressed under phosphorus limited conditions (Arx et al., 2023; Sosa et al., 2019). The *phnCDEFGHIJKLMNOP* operon is capable of degrading several types of phosphonates, however, the *phnJ* gene is specifically responsible for encoding a protein that demethylates methylphosphonates (Sosa et al., 2019). The C-P bond attaching the alkyl group to the phosphonate is cleaved, resulting in phosphorus acquisition and methane formation (Kamat et al., 2011).

The *phnJ* gene can therefore be used as a marker to determine if microbes are capable of methylphosphonate degradation (Arx et al., 2023; Sosa et al., 2019). This aerobic demethylation process and gene marker have been documented in pelagic cyanobacteria across the globe using marine metagenomes (Sosa et al., 2019; Repeta et al., 2016; Arx et al., 2023). However, little is known about the metagenomic potential of benthic cyanobacteria in salt marsh microbial mats to express the *phnJ* gene. This chapter will explore whether benthic

cyanobacteria have the metabolic genes (i.e. *phnJ*) necessary for aerobic methanogenesis using methylphosphonate under phosphorus limitation.

Methods:

C-P Lyase Gene Analysis

Reference *phnJ* sequences for cyanobacteria species were reported by Arx et al. (2023; accession codes MBS9773392 and NER28171.1). Both reference sequences are from metagenome-assembled genomes (MAGs) of pelagic cyanobacteria that expressed the *phnJ* gene. These reference sequences were input into the National Center for Biotechnology Information (NCBI) database to find their respective FASTA amino acid sequences.

Reference amino acid sequences were input into NCBI's basic local alignment search tool (BLAST). BLAST-p was used to compare the reference FASTA sequences to cyanobacteria species (taxonomic identifier: 1117). Sequences producing significant alignments were screened to determine if the cyanobacteria species was from a microbial mat sample. Percent identities above 60% are included in the screening.

Microbial Mat MAG Analysis

Wong et al. (2018) identified cyanobacteria MAGs from intertidal microbial mats in Shark Bay, Australia. Shark Bay is home to one of the most expansive microbial mat systems and undergoes daily tidal fluctuations, making it a useful comparison to other intertidal environments, such as salt marshes (Wong et al., 2018).

High-quality cyanobacteria MAGs were selected and annotated to identify whether the *phnJ* gene was present. tBLASTn was used to align *phnJ* reference sequences (accession codes: MBS9773392 and NER28171.1) to the selected high-quality Shark Bay cyanobacteria MAG containing the *phnJ* gene (accession code: Smooth.098). Query results were matched to the corresponding annotated contig, or the set of overlapping DNA sequences.

Results and Discussions:

Cyanobacteria phnJ Gene Presence

The initial cyanobacteria *phnJ* BLAST search produced 251 sequences of significant

alignments. Of the 251 queried sequences, 41 sequences have percent identity values above

60% and only one sequence (accession number TVQ21588.1) is from a microbial mat sample

(Table 2). The remaining sequences are either pelagic, sedimentary, or isolated from cultures.

The most common cyanobacteria genus in the query results is *Trichodesmium*, but there

is a wide range of 16 cyanobacteria genera in total (Figure 5, Table 2). *Trichodesmium* is also

the genus with the highest percent identity values, followed by *Symploca* and *Merismopedia*

(Figure 6). Most query results originate from pelagic sources. Genera that originate from

multiple sequence sources tend to have similar percent identity values regardless of sequence

source (Figure 6, Table 2).

Leptolyngbya is the sole cyanobacteria genus that originates from a microbial mat

sample (Figure 5, Table 2). This microbial mat was sampled from an alkaline soda lake located

on Cariboo Plateau in British Columbia, Canada. These lakes are characterized by high salinity

and pH, making soda lakes a comparable environment to salt marsh systems as they both can

harbor extremophilic and halophilic mat-forming cyanobacteria (Zorz et al., 2019).

Table 2: Query results of the *phnJ* gene BLAST search against cyanobacteria taxa ID 1117. Results are ordered by increasing e-value. Sequence source was identified from the original study each sequence was associated with.

| Number	Genus	Query Cover	E-Value	% Identity	Sequence Source
1	*Trichodesmium*	100	0	100	Culture
2	*Trichodesmium*	100	0	99.37	Pelagic
3	*Trichodesmium*	100	0	99.05	Pelagic
4	*Trichodesmium*	100	0	97.46	Pelagic
5	*Symploca*	96	0	93.75	Pelagic
6	*Symploca*	96	0	93.75	Pelagic
7	*Symploca*	96	0	93.42	Pelagic
8	*Rivularia*	91	0	89.58	Pelagic
9	*Calothrix*	96	0	83.65	Culture
10	*Rivularia*	95	0	83.72	Pelagic
11	*Mastigocoleus*	90	2.0E-178	82.81	Coastal Sediment
12	*Mastigocoleus*	90	3.0E-175	81.75	Coastal Sediment
13	*Mastigocoleus*	90	1.0E-174	81.40	Unknown
14	*Mastigocoleus*	90	3.0E-174	81.34	Unknown
15	*Stenomitos*	87	2.0E-173	81.95	Terrestrial
16	*Pleurocapsa*	89	1.0E-172	81.91	Unknown
17	*Synechococcus*	89	1.0E-172	81.91	Terrestrial
18	*Scytonema*	89	2.0E-171	80.21	Unknown
19	*Scytonema*	89	2.0E-170	80.21	Terrestrial
20	*Nostoc*	89	2.0E-170	80.57	Unknown
21	*Nostoc*	89	3.0E-170	80.14	Unknown
22	*Nostoc*	89	3.0E-169	79.86	Terrestrial
23	*Chroococcidiopsidaceae*	92	3.0E-166	75.00	Terrestrial
24	*Rippkaea*	89	3.0E-165	76.87	Unknown
25	*Iningainema*	89	5.0E-165	79.08	Unknown
26	*Crocosphaera*	87	2.0E-162	77.98	Unknown
27	*Crocosphaera*	88	3.0E-159	76.43	Coastal Sediment
28	*Crocosphaera*	86	5.0E-159	77.94	Coastal Sediment
29	*Crocosphaera*	86	2.0E-158	78.68	Unknown
30	*Trichodesmium*	62	1.0E-139	97.47	Pelagic
31	*Trichodesmium*	51	7.0E-110	96.93	Pelagic
32	*Merismopedia*	50	1.0E-105	93.75	Pelagic
33	*Trichodesmium*	34	4.0E-76	98.18	Pelagic
34	*Trichodesmium*	34	1.0E-75	92.27	Pelagic
35	*Trichodesmium*	33	4.0E-73	98.11	Pelagic
36	*Trichodesmium*	31	7.0E-61	97.96	Pelagic
37	*Trichodesmium*	29	4.0E-58	97.85	Pelagic
38	*Merismopedia*	28	9.0E-58	91.21	Pelagic
39	*Trichodesmium*	29	1.0E-57	96.77	Pelagic
40	*Leptolyngbya*	35	1.0E-43	60.18	Microbial Mat
41	*Calothrix*	20	7.0E-33	84.13	Culture
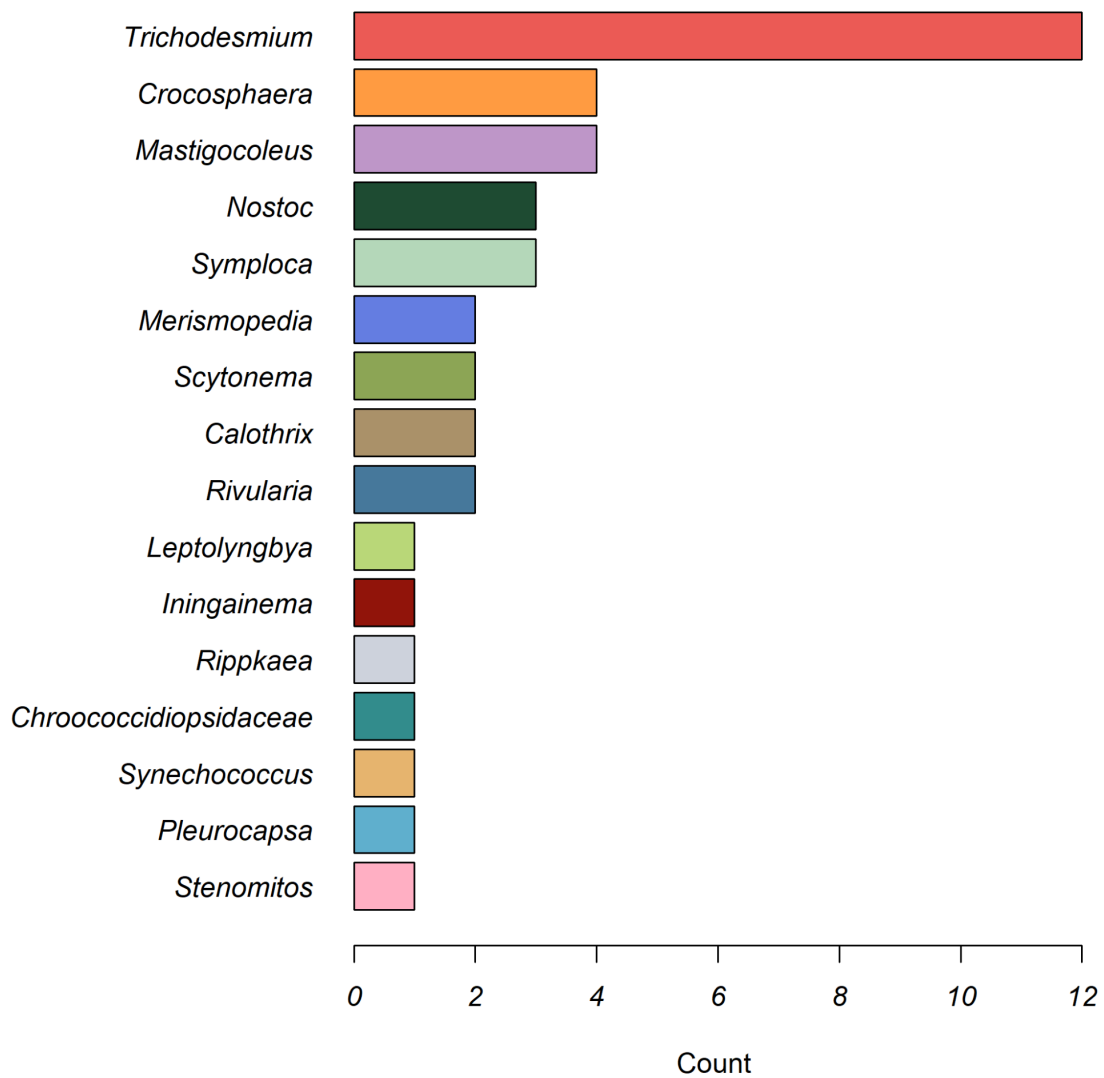
Figure 5: Counts of each cyanobacteria genus that were returned from the *phnJ* gene BLAST search. Counts represent how many times a genus appeared in the query results for genera that had percent identity values above 60%. Colors of genera match those in Figure 6.
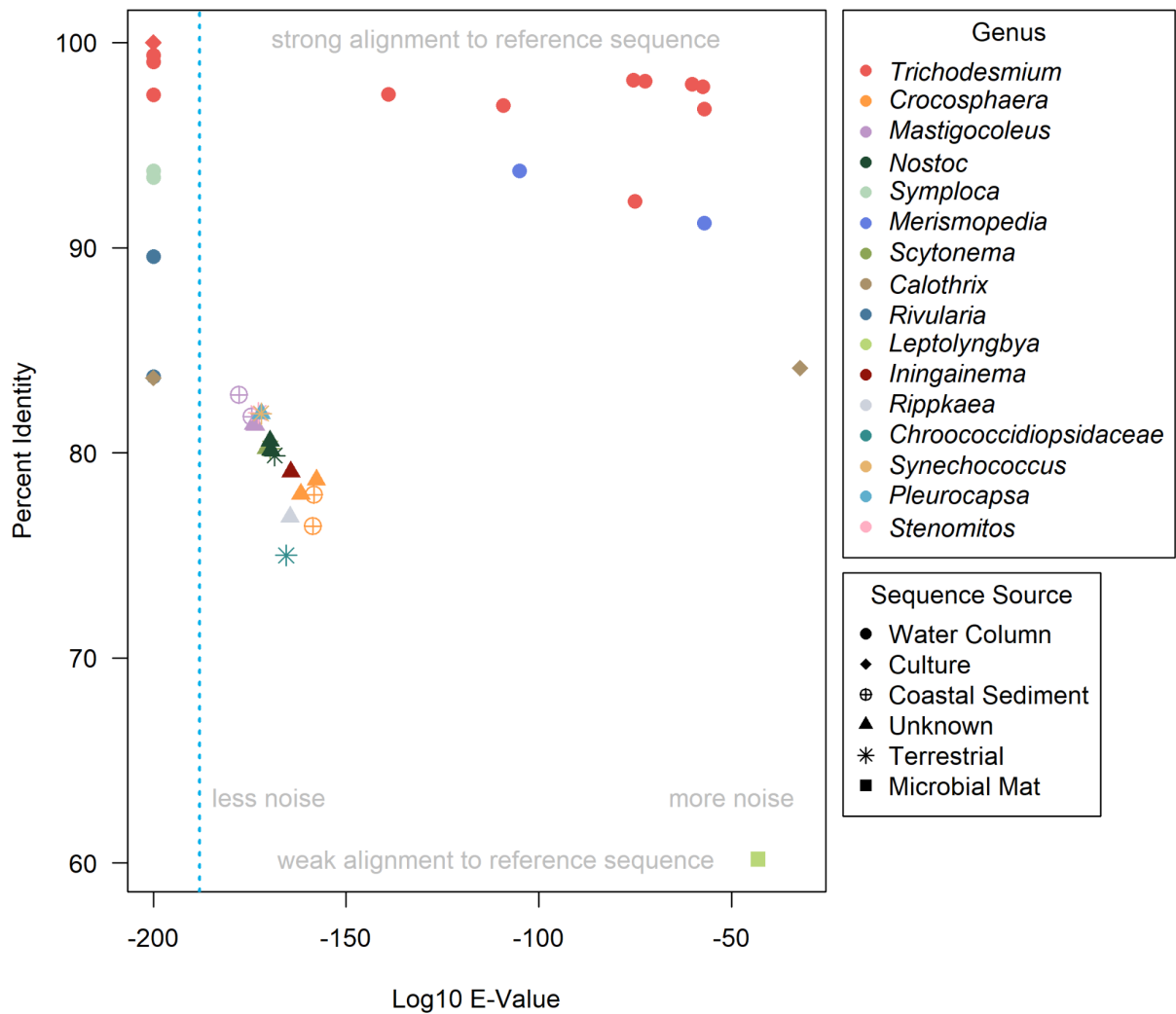
Figure 6: Percent identity values of cyanobacteria sequences that were returned from the *phnJ* gene BLAST search plotted along with their respective $\log_{10}$ e-value scores. Only percent identity values above 60% are included. The blue dotted line separates e-values of zero, as they are plotted as 1.0E-200 to avoid undefined $\log_{10}$ of zero errors (see Table 2 for full list of e-values).

Shark Bay MAG Alignment

The Shark Bay MAG analysis produced unique percent identity values when the high-quality cyanobacteria MAG was aligned with the cyanobacteria *phnJ* gene reference sequences. Reference sequences MBS9773392.1 and NER28171.1 have percent identity values of 52.92% and 52.55% when aligned with the high-quality cyanobacteria MAG (Table 3).

The query results also match both of these reference sequences to contig_101_618847, which

Wong et al. (2018) annotated as a polysaccharide export protein.

Table 3: Query results of Smooth.098 sequence *tBLASTn* alignment to reference sequences
MBS9773392.1 and NER28171.1. Results aligned to contig_101_618847, annotated by Wong et al.
(2018) as a polysaccharide export protein.

Subject	Reference	Query Cover	E-Value	% Identity
Smooth.098	MBS9773392.1	86	1.0E-98	52.92
Smooth.098	NER28171.1	89	4.0E-99	52.55

Conclusions:

The cyanobacteria genera identified from the *phnJ* gene BLAST sequence results

represent a wide range of genera and sequence sources from around the world. A mix of mainly

water column and terrestrial genera show that the *phnJ* gene is found in a variety of

environments and species. However, there is separation in percent identity values between

pelagic and benthic genera. Sequences that originate from water column samples have the

highest percent identity values ranging from 83.72% to 100% identity. Coastal and terrestrial

sequences have percent identity values ranging from 75% to 82.81% identity (Table 2). This

separation in percent identity values could be because the reference *phnJ* sequences

(MBS9773392.1 and NER28171.1) are from the genera *Trichodesmium* and *Symploca*,

respectively, both of which are marine pelagic species (Conover et al., 2021; Leao, 2019)

Although only one of the sequences (accession code: TVQ21588.1) originates from a

microbial mat, this mat is from an inland freshwater lake system, not a salt marsh. This

Leptolyngbya sequence also has the lowest percent identify value (60.18%) when compared

with the reference sequences and the second highest e-value (1.0E-43) (Table 2). The low

percent identity value indicates there is weaker alignment to the reference sequence, whereas

the high e-value indicates that there is more random background noise associated with that sequence (Figure 6). This makes the microbial mat sequence a lower-quality sequence compared to the high percent identity and low e-value sequences.

When the reference sequences are aligned with the Shark Bay microbial mat MAG, the percent identity values of the alignment are 52.92% and 52.55% (Table 3). These values are similar to the 60.18% identity score of the microbial mat sequence from the cyanobacteria *phnJ* BLAST results, possibly indicating that microbial mat cyanobacteria sequences have comparable sequences.

Intertidal microbial mat cyanobacteria may express the *phnJ* gene and contribute to coastal methane production through aerobic methanogenesis (Wong et al., 2018). It is also possible that cyanobacteria present in microbial mats in freshwater lakes, hot springs, and volcanic terrains may express the *phnJ* gene (Zorz et al., 2019; Wang et al., 2017; Hadland et al., 2024). Under phosphorus limited conditions, methane production may occur from these terrestrial microbial mat systems utilizing the C-P lyase demethylation pathway in addition to the known pelagic cyanobacteria species that express the *phnJ* gene.

References:

Arx, J. N. von, Kidane, A. T., Philippi, M., Mohr, W., Lavik, G., Schorn, S., Kuypers, M. M. M. & Milucka, J. (2023). Methylphosphonate-driven methane formation and its link to primary production in the oligotrophic North Atlantic. *Nature Communications*, *14*(1), 6529. https://doi.org/10.1038/s41467-023-42304-4

Conover, A. E., Morando, M., Zhao, Y., Semones, J., Hutchins, D. A. & Webb, E. A. (2021). Alphaproteobacteria facilitate *Trichodesmium* community trimethylamine utilization. *Environmental Microbiology*, *23*(11), 6798–6810. https://doi.org/10.1111/1462-2920.15773

Duhamel, S., Diaz, J. M., Adams, J. C., Djaoudi, K., Steck, V. & Waggoner, E. M. (2021). Phosphorus as an integral component of global marine biogeochemistry. *Nature Geoscience*, *14*(6), 359–368. https://doi.org/10.1038/s41561-021-00755-8

Hadland, N., Hamilton, C. W. & Duhamel, S. (2024). Young volcanic terrains are windows into early microbial colonization. *Communications Earth & Environment*, *5*(1), 114. https://doi.org/10.1038/s43247-024-01280-3

Kamat, S. S., Williams, H. J. & Raushel, F. M. (2011). Intermediates in the transformation of phosphonates to phosphate by bacteria. *Nature*, *480*(7378), 570–573. https://doi.org/10.1038/nature10622

Leao, T. F. (2019). Comparative Genomics and Genome Mining Insights into Natural Product Rich Marine Cyanobacteria. *University of California San Diego Dissertation Archive*.

Metcalf, W. W., Griffin, B. M., Cicchillo, R. M. & Donk, W. A. van der. (2012). Synthesis of methylphosphonic acid by marine microbes: a source for methane in the aerobic ocean. *Science Magazine*. https://doi.org/10.1126/science.1219875

Repeta, D. J., Ferrón, S., Sosa, O. A., Johnson, C. G., Repeta, L. D., Acker, M., DeLong, E. F. & Karl, D. M. (2016). Marine methane paradox explained by bacterial degradation of dissolved organic matter. *Nature Geoscience*, *9*(12), 884–887. https://doi.org/10.1038/ngeo2837

Sosa, O. A., Repeta, D. J., DeLong, E. F., Ashkezari, M. D. & Karl, D. M. (2019). Phosphate-limited ocean regions select for bacterial populations enriched in the carbon–phosphorus lyase pathway for phosphonate degradation. *Environmental Microbiology*, *21*(7), 2402–2414. https://doi.org/10.1111/1462-2920.14628

Wang, Q., Dore, J. E. & McDermott, T. R. (2017). Methylphosphonate metabolism by Pseudomonas sp. populations contributes to the methane oversaturation paradox in an oxic freshwater lake. *Environmental Microbiology*, *19*(6), 2366–2378. https://doi.org/10.1111/1462-2920.13747

White, A. K. & Metcalf, W. W. (2007). Microbial metabolism of reduced phosphorus compounds. *Annual Review of Microbiology*, *61*(1), 379–400. https://doi.org/10.1146/annurev.micro.61.080706.093357

Wong, H. L., White, R. A., Visscher, P. T., Charlesworth, J. C., Vázquez-Campos, X. & Burns, B. P. (2018). Disentangling the drivers of functional complexity at the metagenomic level in Shark Bay microbial mat microbiomes. *The ISME Journal*, *12*(11), 2619–2639. https://doi.org/10.1038/s41396-018-0208-8

Zorz, J. K., Sharp, C., Kleiner, M., Gordon, P. M. K., Pon, R. T., Dong, X. & Strous, M. (2019). A shared core microbiome in soda lakes separated by large distances. *Nature Communications*, *10*(1), 4230. https://doi.org/10.1038/s41467-019-12195-5

CHAPTER 4

OVERARCHING CONCLUSIONS

<u>Major Outcomes:</u>

Salt Marsh Aerobic Methanogenesis

Methane was produced under light conditions when methylphosphonate compounds were present. Light treatment methanogenesis could theoretically be caused by aerobic demethylation of MPn compounds by salt marsh cyanobacteria as a means of acquiring essential nutrients under nutrient limited conditions, but this process occurs only if the mats are under oxic conditions (Arx et al., 2023; Bižić-Ionescu et al., 2019; Wang et al., 2021). Although it cannot be concluded that this alternative aerobic methanogenesis pathway was used to produce methane as a reaction byproduct, as most methane concentrations were below the detection limit and dark treatment methane production indicates the vials went anoxic at a certain point, this study has implications for salt marsh methane dynamics. Controls of coastal wetland nutrient regimes and methane emissions are uncertain in a changing climate (Capooci et al., 2024). Furthermore, aerobic methanogenesis in salt marsh systems has not been studied before, even though salt marshes are globally essential and contribute to the largest terrestrial methane source (Tiwari et al., 2020). This study provides insights into these limiting factors of salt marsh research.

Oxic Methanogenesis Gene Markers

The results of the BLAST analysis show that several genera of cyanobacteria have the metabolic genes necessary for aerobic methanogenesis utilizing methylphosphonate. The *phnJ* gene is present in several terrestrial and aquatic cyanobacteria genera, indicating that these cyanobacteria are capable of expressing the C-P lyase enzyme under phosphorus limited conditions (Repeta et al., 2016). The presence of the *phnJ* gene means that these cyanobacteria can degrade methylphosphonates to acquire phosphorus, thereby producing

methane as a reaction byproduct (Sosa et al., 2019). The *phnJ* gene can therefore be used as a marker in metagenomic studies to distinguish microorganisms that can express the C-P lyase enzyme. Metagenomes of cyanobacteria are relatively scarce in public repositories, and only a handful of high-quality microbial mat metagenomes exist (Leao, 2019; Armitage et al., 2012). This work explores the gaps in coastal metagenome research and aims to highlight the use of gene markers in methane production studies.

Improvements to Experimental Design:

The experiment investigating whether coastal cyanobacteria in microbial mats produce methane under nutrient-limited conditions should be repeated with more robust microbial mat samples. The mat samples used in this experiment were not clearly stratified, and it was therefore difficult to delineate the mat from the underlying sediment. The experiment should also be repeated using an oxygen microelectrode in order to determine the oxygen levels within each vial and the exact time point that the vials went anoxic. A methanogenesis inhibitor and a photosynthesis inhibitor should be included as controls in future experiments to determine whether methane was produced from other microbes within the microbial mat or the sediment. DNA extraction and shotgun sequencing should also be done in future experiments to determine the community composition and to produce high-quality MAGs of microbial mat microorganisms, specifically cyanobacteria species.

The creation of microbial mat MAGs could be useful for the experiment investigating whether cyanobacteria in intertidal microbial mats have the metabolic genes necessary for aerobic methanogenesis using methylphosphonate under nutrient limitation. High-quality cyanobacteria MAGs from a salt marsh microbial mat could be used in a BLAST analysis to identify whether the *phnJ* gene is present. If the gene is present, the cyanobacteria MAG could be used as a reference sequence for future intertidal metagenomic studies.

Relevance to Global Methane Regulation:

The potential for coastal microorganisms to use alternative aerobic methanogenic pathways has implications for global methane studies. Salt marsh ecosystems represent approximately 0.3% of the world's total land area and are a critical component in methane cycling (Mcowen et al., 2017; Tiwari et al., 2020). However, much uncertainty surrounds the controls of coastal methane emissions and no research has been done to investigate cyanobacteria-mediated aerobic methanogenesis in microbial mats (Capooci et al., 2024).

It is important to constrain how these missing factors impact emissions estimates of the global methane budget. An underrepresentation of natural methane emissions and a lack of understanding of coastal methane dynamics can hinder efforts to preserve these critical intertidal habitats and wetland systems (Saunois et al., 2020; Bastviken et al., 2011). Furthering our evaluations of the global methane budget will decrease uncertainties and lead to the enactment of policy measures that strive to combat climate change effects in a warming planet.

References:

Arx, J. N. von, Kidane, A. T., Philippi, M., Mohr, W., Lavik, G., Schorn, S., Kuypers, M. M. M. & Milucka, J. (2023). Methylphosphonate-driven methane formation and its link to primary production in the oligotrophic North Atlantic. *Nature Communications*, *14*(1), 6529. https://doi.org/10.1038/s41467-023-42304-4

Armitage, D. W., Gallagher, K. L., Youngblut, N. D., Buckley, D. H. & Zinder, S. H. (2012). Millimeter-scale patterns of phylogenetic and trait diversity in a salt marsh microbial mat. *Frontiers in Microbiology*, *3*, 293. https://doi.org/10.3389/fmicb.2012.00293

Bastviken, D., Tranvik, L. J., Downing, J. A., Crill, P. M. & Enrich-Prast, A. (2011). Freshwater Methane emissions offset the continental carbon sink. *Science*, *331*(6013), 50–50. https://doi.org/10.1126/science.1196808

Bižić-Ionescu, M., Ionescu, D., Günthel, M., Tang, K. W. & Grossart, H.-P. (2019). *Biogenesis of Hydrocarbons*. 379–400. https://doi.org/10.1007/978-3-319-78108-2_10

Capooci, M., Seyfferth, A. L., Tobias, C., Wozniak, A. S., Hedgpeth, A., Bowen, M., Biddle, J. F., McFarlane, K. J. & Vargas, R. (2024). High methane concentrations in tidal salt marsh soils: Where does the methane go? *Global Change Biology*, *30*(1), e17050. https://doi.org/10.1111/gcb.17050

Leao, T. F. (2019). Comparative Genomics and Genome Mining Insights into Natural Product Rich Marine Cyanobacteria. *University of California San Diego Dissertation Archive*.

Mcowen, C., Weatherdon, L., Bochove, J., Sullivan, E., Blyth, S., Zockler, C., Stanwell-Smith, D., Kingston, N., Martin, C., Spalding, M., Fletcher, S. (2017). A global map of saltmarshes. *Biodiversity Data Journal*. 5, e11764. https://doi.org/10.3897/BDJ.5.e11764

Repeta, D. J., Ferrón, S., Sosa, O. A., Johnson, C. G., Repeta, L. D., Acker, M., DeLong, E. F. & Karl, D. M. (2016). Marine methane paradox explained by bacterial degradation of dissolved organic matter. *Nature Geoscience*, *9*(12), 884–887. https://doi.org/10.1038/ngeo2837

Saunois, M., Stavert, A. R., Poulter, B., Bousquet, P., Canadell, J. G., Jackson, R. B., Raymond, P. A., Dlugokencky, E. J., Houweling, S., Patra, P. K., Ciais, P., Arora, V. K., Bastviken, D., Bergamaschi, P., Blake, D. R., Brailsford, G., Bruhwiler, L., Carlson, K. M., Carrol, M., … Zhuang, Q. (2020). The global methane budget 2000–2017. Earth System Science Data, 12(3), 1561–1623. https://doi.org/10.5194/essd-12-1561-2020

Sosa, O. A., Repeta, D. J., DeLong, E. F., Ashkezari, M. D. & Karl, D. M. (2019). Phosphate-limited ocean regions select for bacterial populations enriched in the carbon–phosphorus lyase pathway for phosphonate degradation. *Environmental Microbiology*, *21*(7), 2402–2414. https://doi.org/10.1111/1462-2920.14628

Tiwari, S., Singh, C., Singh, J.S. (2020). Wetlands: A Major Natural Source Responsible for Methane Emission. Restoration of Wetland Ecosystem: A Trajectory Towards a Sustainable Environment. Springer. https://doi.org/10.1007/978-981-13-7665-8_5

Wang, Q., Alowaifeer, A., Kerner, P., Balasubramanian, N., Patterson, A., Christian, W., Tarver, A., Dore, J. E., Hatzenpichler, R., Bothner, B. & McDermott, T. R. (2021). Aerobic bacterial methane synthesis. *Proceedings of the National Academy of Sciences*, *118*(27), e2019229118. https://doi.org/10.1073/pnas.2019229118

Normalized Difference Vegetation Index (NDVI) Analysis:

Figure S1: Normalized Difference Vegetation Index (NDVI) was calculated for the area around Skidaway Island, Georgia, USA. Spectrometric data taken on August 14th, 2023 by NASA's Landsat 8 Earth Observation Satellite were selected for analysis. ArcGIS Pro was used to calculate NDVI using the Landsat 8 near infrared and red band data. Areas of higher vegetation density are denoted by darker colors (values of +1), whereas areas of lower vegetation density are denoted by lighter colors (values of -1). The sampling location for microbial mat collection is highlighted.

Geochemical Analysis Information:

Table S1: Geochemical parameters measured during the time-series incubation experiment. Samples were analyzed for methane (CH_4), ammonium (NH_4), nitrite (NO_2^-), the sum of nitrate and nitrite (NO_x^-), phosphate (PO_4^{3-}), total dissolved phosphate (TDP), total dissolved nitrogen (TDN), and dissolved organic carbon (DOC). Instruments used and detection limits are included for all geochemical parameters.

Parameter	Instrument	Detection Limit
CH_4	SRI 8610C Gas Chromatograph with FID Detector	1 nmol/L
NH_4	Shimadzu UV-1601 Spectrophotometer	0.1 μmol/L
NO_2^-	Shimadzu UV-1601 Spectrophotometer	0.1 μmol/L
NO_x^-	Shimadzu UV-1601 Spectrophotometer	0.1 μmol/L
PO_4^{3-}	Shimadzu UV-1601 Spectrophotometer	0.1 μmol/L
TDP	Shimadzu UV-1601 Spectrophotometer	0.1 μmol/L
TDN	Shimadzu TOC-Vcph	1 μmol/L
DOC	Shimadzu TOC-Vcph	1 μmol/L